HHS Public Access

Author manuscript

Eur Radiol. Author manuscript; available in PMC 2024 August 01.

Published in final edited form as:

Eur Radiol. 2024 August ; 34(8): 5204–5214. doi:10.1007/s00330-023-10548-9.

Wall permeability on magnetic resonance imaging is associated with intracranial aneurysm symptoms and wall enhancement

Qichang Fu[1], **Yi Zhang**[1], **Yong Zhang**[1], **Chao Liu**[2], **Jinyi Li**[2], **Meng Wang**[3], **Haiyang Luo**[4], **Jinxia Zhu**[5], **Feifei Qu**[5], **Mahmud Mossa-Basha**[6], **Sheng Guan**[2], **Jingliang Cheng**[1,*], **Chengcheng Zhu**[6]

[1]Department of Magnetic Resonance, The First Affiliated Hospital of Zhengzhou University, 1St Construction of E Rd, Two-Seven Districts, Zhengzhou 450052, China.

[2]Department of Interventional Neuroradiology, The First Affiliated Hospital of Zhengzhou University, Zhengzhou, China.

[3]Department of Neurosurgery, The First Affiliated Hospital of Zhengzhou University, Zhengzhou, China.

[4]Department of Neurology, The First Affiliated Hospital of Zhengzhou University, Zhengzhou, China.

[5]MR Collaboration, Siemens Healthineers Ltd, Beijing, China.

[6]Department of Radiology, University of Washington School of Medicine, Seattle, WA, USA.

Abstract

[*]Correspondence: Jingliang Cheng, fccchengjl@zzu.edu.cn.

Guarantor

The scientific guarantor of this publication is Jingliang Cheng.

Supplementary information

The online version contains supplementary material available at https://doi.org/10.1007/s00330-023-10548-9.

Conflict of interest

Two of the authors of this manuscript (Jinxia Zhu and Feifei Qu) are employees of Siemens Healthineers. The remaining authors declare no relationships with any companies whose products or services may be related to the subject matter of the article.

Statistics and biometry

Chunhua Song (a medical statistician from Zhengzhou University) kindly provided statistical advice for this manuscript.

Informed consent

Written informed consent was obtained from all subjects (patients) in this study.

Ethical approval

The approval of the ethics committee of the First Affiliated Hospital of Zheng-zhou University was obtained (Ethics No. ss-2018–11).

Study subjects or cohorts overlap

Some study subjects or cohorts have been previously reported in “Qualitative and Quantitative Wall Enhancement on Magnetic Resonance Imaging Is Associated With Symptoms of Unruptured Intracranial Aneurysms. *Stroke* (1970) 52:213–222” and “Evaluation of the Instability of Intracranial Aneurysms Wall by Dynamic Contrast-enhanced Magnetic Resonance Imaging and Vessel Wall Imaging” by the International Society for Medical Magnetic Resonance Annual Meeting (ISMRM 2022).

Methodology

- prospective
- case-control study
- performed at one institution

Objectives—Wall remodeling and inflammation accompany symptomatic unruptured intracranial aneurysms (UIAs). The volume transfer constant (K^{trans}) of dynamic contrast-enhanced magnetic resonance imaging (DCE-MRI) reflects UIA wall permeability. Aneurysmal wall enhancement (AWE) on vessel wall MRI (VWI) is associated with inflammation. We hypothesized that K^{trans} is related to symptomatic UIAs and AWE.

Methods—Consecutive patients with UIAs were prospectively recruited for 3-T DCE-MRI and VWI from January 2018 to March 2023. UIAs were classified as asymptomatic and symptomatic if associated with sentinel headache or oculomotor nerve palsy. K^{trans} and AWE were assessed on DCE-MRI and VWI, respectively. AWE was evaluated using the AWE pattern and wall enhancement index (WEI). Spearman's correlation coefficient and univariate and multivariate analyses were used to assess correlations between parameters.

Results—We enrolled 82 patients with 100 UIAs (28 symptomatic and 72 asymptomatic). The median K^{trans} (2.1 versus 0.4 min^{-1}; $p < 0.001$) and WEI (1.5 versus 0.4; $p < 0.001$) were higher for symptomatic aneurysms than for asymptomatic aneurysms. K^{trans} (odds ratio [OR]: 1.60, 95% confidence interval [95% CI]: 1.01–2.52; $p = 0.04$) and WEI (OR: 3.31, 95% CI: 1.05–10.42; $p = 0.04$) were independent risk factors for symptomatic aneurysms. K^{trans} was positively correlated with WEI (Spearman's coefficient of rank correlation (rs) = 0.41, $p < 0.001$). The combination of K^{trans} and WEI achieved an area under the curve of 0.81 for differentiating symptomatic from asymptomatic aneurysms.

Conclusions—K^{trans} may be correlated with symptomatic aneurysms and AWE. K^{trans} and WEI may provide an additional value than the PHASES score for risk stratification of UIAs.

Clinical relevance statement—The volume transfer constant (K^{trans}) from DCE-MRI perfusion is associated with symptomatic aneurysms and provides additional value above the clinical PHASES score for risk stratification of intracranial aneurysms.

Keywords

Intracranial aneurysm; Magnetic resonance imaging; Vessel wall; Inflammation; Permeability

Introduction

Intracranial aneurysms (IAs) occur in 3–5% of adults, and rupture can lead to fatal subarachnoid hemorrhage (SAH) [1]. However, evaluating IA rupture risk remains challenging, and traditional risk factors, including aneurysm size, location, hypertension, and other factors, only achieve moderate performance in risk stratification of IAs [2, 3]. The instability of the IA wall is closely associated with aneurysm rupture. The rupture risk of symptomatic aneurysms is 4.4 times greater than that of asymptomatic aneurysms [4]. Symptoms of aneurysms might help identify the unstable state of the aneurysm wall before it ruptures [5].

IA wall instability is accompanied by remodeling and inflammation [6], and IA wall remodeling may lead to micro-perforations [7] accompanied by changes in permeability. Novel imaging markers of aneurysm wall, including aneurysmal wall enhancement (AWE, marker of inflammation) on vessel wall MRI (VWI) [8] and the wall permeability (volume

transfer constant, K^{trans}) of dynamic contrast-enhanced magnetic resonance imaging (DCE-MRI) [9], have been investigated recently, showing promise in differentiating the unstable state of the aneurysm wall [10, 11]. Small sample sizes have limited previous studies on the permeability of aneurysm walls [10, 12]. Prior investigation has also not addressed whether K^{trans} can provide additional value above traditional risk factors in differentiating symptomatic IAs. Furthermore, it is important to consider the potential existence of AWE in the stable state of the aneurysm wall, as this may decrease the reliability of using AWE as a biomarker specifically for the unstable state of the aneurysm wall [13–15]. To enhance the accuracy of identifying the unstable state of the aneurysm wall, incorporating K^{trans} analysis from DCE-MRI may offer valuable supplementary data. We hypothesize that K^{trans} is associated with symptomatic aneurysms and AWE.

Materials and methods

Subjects

With the approval of the ethics committee of the First Affiliated Hospital of Zhengzhou University (Ethics No. ss-2018–11), consecutive patients with unruptured intracranial aneurysms (UIAs) were prospectively recruited and underwent 3-T DCE-MRI and VWI from January 2018 to March 2023 at a tertiary care center. UIAs are classified into symptomatic and asymptomatic aneurysms. Figure 1 shows the flowchart for patient selection.

Inclusion criteria were as follows: (1) asymptomatic aneurysms without evidence of current or previous rupture, including no history of SAH; (2) UIAs in patients who were symptomatic with the following criteria: (i) sentinel headache (development of a sudden and severe headache on the ipsilateral side of the aneurysm within 2 weeks of admission without prior history of headache within the previous 5 years) or (ii) oculomotor nerve palsy (sudden headache with one or several symptoms of pupillary light reflex disappearing, ptosis, or extraocular myoparalysis on the ipsilateral side of the aneurysm within 1 month prior to admission); and (3) UIAs underwent DCE-MRI and VWI before any intervention.

The exclusion criteria were as follows: (1) dissecting aneurysms, fusiform aneurysms, or infundibulum in place of aneurysms; (2) unsatisfactory IA image quality due to motion artifacts; (3) symptomatic patients of sentinel headache with multiple UIAs (due to uncertainty of which UIA caused the patient’s specific symptoms); and (4) ruptured IAs (CT/MRI confirmed SAH and CTA/MRA/DSA found IAs).

The patients approved the content of the study.

Imaging protocol

All patients were scanned on a 3-T MR system (MAG-NETOM Prisma, Siemens Healthcare) with 64-channel neurovascular coils in the MRI department of our hospital. Three-dimensional (3D) time-of-flight magnetic resonance angiography (TOF MRA) was acquired in the axial plane for aneurysm localization. DCE-MRI was obtained with intravenous administration of 0.1 mmol/kg Gd-DTPA (Magnevist; Bayer HealthCare Pharmaceuticals). VWI included a 3D T1-weighted sampling perfection with application-

optimized contrasts using different flip angle evolutions (SPACE) sequences, which was performed before and after 10 min of intravenous administration of Gd-DTPA. The scanning parameters were as follows: (1) TOF MRA: TR/TE: 20.0/3.7 ms, the field of view (FOV): 200 × 80 mm^2, voxel size: 0.6 × 0.6 × 0.6 mm^3, and scan time: 2 min 29 s; (2) B1 mapping using turbo-FLASH was acquired for T1 map correction: TR/TE: 8980/2.54 ms, FOV: 280 × 175 mm^2, voxel size: 4.4 × 4.4 × 2.0 mm^3, and scan time: 18 s; T1 mapping was conducted before contrast injection using a variable flip angle (VFA) technique: TR/TE: 5.32/2.42 ms, FOV: 240 × 210 mm^2, 6 flip angles (FA): 3°, 5°, 8°, 10°, 13°, 15°, voxel size: 0.6 mm × 0.6 × 3.0 mm^3, and scan time: 1 min 38 s; quantitative T1 map was automatically generated inline after data acquisition; multi-phase DCE-MRI was acquired using a volumetric interpolated breathhold (VIBE) sequence: TR/TE = 2.84/0.80 ms, FOV: 190 × 190 mm^2, FA: 15°, voxel size: 0.7 × 0.7 × 3.0 mm^3, 80 measurements (each measurement time: 7.5 s), and scan time: 9 min 59 s. (3) 3D T1-weighted SPACE sequence parameters were TR/TE: 900/15 ms, FOV: 200 × 200 mm^2, voxel size: 0.6 × 0.6 × 0.6 mm^3, echo train duration: 254 ms, and scan time: 7 min 36 s.

Evaluation methods for K^{trans}, AWE pattern, and rupture risk of IAs

Two neuroradiologists (with 10 and 5 years of neuroimaging diagnosis experience) obtained the K^{trans} of the IA wall on VWI by independent blinded analysis of the DCE-MRI images using Siemens Syngo.via workstation TISSUE 4D software (Fig. 2). DCE-MRI and VWI of IAs were loaded into Tissue 4D software for Siemens Syngo. via workstations. The software used motion correction to correct position deviation of the DCE-MRI between multiple phases caused by involuntary movement of the aneurysm during scanning. The software automatically matched the DCE-MRI with VWI and locked IAs in the fused image. After combining the multi-phase dynamic scanning data with the tissue reference T1 values (measured based on T1 mapping), the raters selected the volume of interest (VOI) of the IAs in the fused image. The software automatically calculated the corresponding DCE-MRI curves on the VOI. In the VOI above, three IA wall slices (top, body, and bottom) on the VWI were selected by the raters, who traced the lumen and outer boundaries of the aneurysmal wall through the optimally displayed angle (coronal, sagittal, or axial based on the specific geometry of the aneurysm). The software automatically calculated the K^{trans} of the corresponding aneurysmal walls on the DCE-MRI in the fusion image. The raters selected the largest K^{trans} for further analysis. The Tofts model was used to quantify the kinetics of the contrast agent leaking through the IA wall:

$$C_t(t) = K^{trans}\left[C_p(t) \otimes e^{\left(-k_{ep} * t\right)}\right]$$

The AWE pattern (AWEP) of the IA walls was evaluated by two senior neuroradiologists (30 and 20 years of neuroimaging diagnostic experience) who independently assessed the VWI in the study by blinded analysis as previously described [5]. The AWEPs on the VWI were qualitatively defined as AWEP 0: no wall enhancement or similar degree of enhancement to the normal arterial wall, AWEP 1: focal wall enhancement, and AWEP 2: circumferential wall enhancement. Focal wall enhancement was defined as involving the

neck, dome, intermediate portion, and/or a bleb, whereas circumferential wall enhancement would involve the entire circumference of the aneurysm on all three slices.

The wall enhancement index (WEI) of the IAs was determined by two neuroradiologists (10 and 5 years of neuroimaging diagnostic experience) who independently evaluated the VWI via Vessel-MASS software (MEDIS, Version: 2014-EXP) as previously described [5]. Detailed information is provided in the WEI analysis of the VWI in the supplemental file. The WEI was measured using the following equation (SI indicates signal intensity):

$$WEI = \frac{\frac{SI\_Wall_{postcontrast}}{SI\_White\,matter_{postcontrast}} - \frac{SI\_Wall_{precontrast}}{SI\_White\,matter_{precontrast}}}{\frac{SI\_Wall_{precontrast}}{SI\_White\,matter_{precontrast}}}$$

The PHASES score [16], which is a commonly used clinical score for the evaluation of aneurysm rupture risk, was recorded by a neuroradiologist. Please refer to the supplementary IA rupture risk analysis file for further details.

Statistical analysis

Data were assessed for normality using the Shapiro-Francia test, and continuous variables were summarized as the means ± standard deviation (SD) or median (interquartile range) as appropriate. Categorical variables are presented as percentages. Interreader agreement of the measured K^{trans} was compared using the concordance correlation coefficient and Bland–Altman analysis. The Cohen k statistic was used for interrater assessment of the AWEP. Spearman's correlation coefficient was used to evaluate the relationships of putative risk factors of aneurysm instability. Multicollinearity testing used the variance inflation factor (VIF) as an assessment criterion. No multicollinearity between components is indicated by a VIF of 1. Moderate multicollinearity is shown by a VIF of 1 to 5, and a VIF of 5 to 10 characterizes high multicollinearity that may be problematic. A VIF of > 10 indicates the unreliability of the regression analysis [17]. Comparisons between groups were conducted using the χ^2 test for categorical variables and the Mann–Whitney U test for continuous variables. The univariate regression analysis included variables with $p < 0.2$ for group comparisons. Variables with $p < 0.05$ in the univariate analysis were further analyzed in the multivariate analysis using backward multiple logistic regression to determine factors independently associated with symptomatic IAs. The logistic mixed regression method was adjusted for individuals who had more than one aneurysm. Receiver operating characteristic (ROC) curves were plotted for independent factors to differentiate symptomatic and asymptomatic aneurysms, and the area under the ROC curves (AUCs) was calculated (null hypothesis of AUC is 0.5). $p < 0.05$ was considered significant, and all p values were 2-sided.

Results

Patient demographics, K^{trans}, and AWE characteristics

From the initial sample of 118 patients with 153 aneu-rysms, 82 patients (mean age 58.2 ± 10.5 years; 70.0% females) with 100 UIAs (median size 5.9 mm [4.0–8.7 mm]; 72 asymptomatic and 28 symptomatic aneurysms) were finally included.

The median K^{trans} was higher for symptomatic IAs than asymptomatic IAs (2.1 versus 0.4 min^{-1}; $p < 0.001$, Table 1, Fig. 3a). AWEP 2 was more common in symptomatic IAs than in asymptomatic IAs (16/28 versus 9/72, $p < 0.001$, Table 1). The median WEI was higher for symptomatic IAs than for asymptomatic IAs (1.5 versus 0.4; $p < 0.001$, Table 1). Figures 4 and 5 show the representative case.

K^{trans} values for AWEP 0, AWEP 1, and AWEP 2 differed significantly ($p < 0.001$) at 0.4 (0.2, 1.1) min^{-1}, 0.9 (0.6, 1.7) min^{-1}, and 3.8 (0.7, 4.0) min^{-1}, respectively. K^{trans} was positively correlated with AWEP, WEI, aneurysm size, and PHASES score (Spearman's coefficient of rank correlation (rs) = 0.45 [95% confidence interval (95% CI), 0.28–0.59], $p < 0.001$; rs = 0.41 [95% CI: 0.23–0.56], $p < 0.001$, Fig. 3b; rs = 0.42 [95% CI: 0.24 to 0.57], $p < 0.001$, Fig. 3c; rs = 0.45 [95% CI: 0.27–0.59], $p < 0.001$, Fig. 3d). The VIF of K^{trans}, size, WEI, and AWEP are 1.41, 1.50, 2.39, and 2.66, respectively, indicating a moderate collinearity unlikely to significantly affect the following multivariate analysis.

Factors associated with symptomatic IAs

Multivariate regression analysis (Table 2) indicated that K^{trans} and WEI were independent risk factors associated with symptomatic aneurysms (odds ratio [OR] = 1.60 for K^{trans} [95% CI, 1.01–2.52], $p = 0.04$; OR = 3.31 for WEI [95% CI, 1.05–10.42], $p = 0.04$, respectively).

The information criterion values of this multivariate regression model are 510.65 (Akaike corrected) and 524.95 (Bayesian). Information criteria are based on the − 2 log pseudo-likelihood (497.69) and are used to compare models. Models with smaller information criterion values fit better.

The ROC (Table 3 and Fig. 6) showed that the AUCs of K^{trans}, WEI, K^{trans} + WEI, size, and PHASES for differentiating symptomatic from asymptomatic IAs were 0.76, 0.76, 0.81, 0.66, and 0.59, respectively. A pairwise comparison of the ROC curves showed statistical differences between K^{trans} and PHASES ($p = 0.01$), WEI and PHASES ($p = 0.03$), K^{trans} + WEI and PHASES ($p < 0.001$), and K^{trans} + WEI and size ($p = 0.02$).

Repeatability

The K^{trans} measurements yielded excellent interobserver agreement (concordance correlation coefficient = 0.84 [95% CI, 0.77–0.89]; Figure S1a) and minimal variability (mean = 0.07 [95% CI, − 0.09 to 0.22], $p = 0.38$; Figure S1b). Interobserver agreement was excellent for identifying AWEP (Cohen $k = 0.80$ [95% CI, 0.70–0.90]) and measuring WEI (concordance correlation coefficient = 0.93 [95% CI, 0.90–0.96]).

Discussion

Our results demonstrated that both K^{trans} and AWE were related to symptomatic aneurysms and that K^{trans} was positively correlated with AWE. We proved that K^{trans} and AWE provide additional value for differentiating symptomatic aneurysms above what traditional risk factors offer alone. To our knowledge, this was the most extensive study to date on symptomatic aneurysms evaluated in combination with DCE-MRI and VWI.

The micro-perforations of the IAs wall are considered the pathogenesis of sentinel headaches [18,19]. The rapid expansion of the IAs wall may lead to oculomotor nerve paralysis [5]. IA wall instability is accompanied by remodeling and inflammation, which may lead to blood leakage [6, 7]. K^{trans} on DCE-MRI can indicate whether the aneurysm wall is permeable to blood [9, 20]. AWE on VWI is associated with inflammation [8, 21–23]. Combining DCE-MRI and VWI to study IAs will allow a better understanding of the instability of the aneurysm wall in regard to permeability and inflammation. The coexistence of AWE and elevated K^{trans} levels within symptomatic aneurysm walls suggests the presence of inflammatory response and increased permeability in unstable aneurysm walls. These findings contribute to enhancing our knowledge regarding the development of AWE in stable aneurysm walls [13].

Recent studies have confirmed that K^{trans} may allow the evaluation of blood leakage in the aneurysmal wall [9, 10, 12, 20]. However, few studies have evaluated the K^{trans} in symptomatic IAs. We showed for the first time that K^{trans} was significantly elevated in symptomatic IAs, suggesting that the unstable state of the aneurysm wall may be accompanied by aneurysmal wall permeability. Previous studies have shown the value of K^{trans} in assessing the risk of aneurysm rupture [10, 12]. A positive correlation has been demonstrated between K^{trans} and aneurysm size [12] and separately between K^{trans} and PHASES score [10]. Here, we report that K^{trans} was an independent risk factor for symptomatic aneurysms and reconfirm that K^{trans} was positively associated with aneurysm size and PHASES score in a larger cohort. Lower wall shear stress and slower blood flow may lead to an inflammatory response in the wall of large IAs [24]. Large aneurysms may have a longer inflammatory response time than small aneurysms [25]. The positive correlation between aneurysm size and K^{trans} suggests that the duration of aneurysm wall inflammation may be related to the increased permeability of the aneurysm wall. The positive correlation between K^{trans} and PHASES score confirms that the higher the permeability of the aneurysm wall, the greater the risk of rupture. Our results also demonstrated that K^{trans} allowed differentiating symptomatic IAs from asymptomatic IAs. K^{trans} may provide additional information on aneurysm wall permeability and contribute to IA risk stratification.

This study further validates the association between AWE and symptomatic aneurysms, similar to findings in prior studies [5, 26, 27]. However, unlike earlier research, we explored the symptomatic aneurysmal wall inflammation and permeability and their relationship by combining AWE and K^{trans}. Unlike previous studies[10], we confirmed a significant positive correlation between AWEP and K^{trans} in a more extensive IA sample set. As a quantitative indicator of AWE, WEI was positively correlated with K^{trans}, consistent with previous

reports [10]. Our study found that symptomatic IAs exhibit simultaneous AWE and K^{trans} increases, suggesting a potential correlation between heightened inflammatory response and increased permeability within unstable aneurysm walls. The inflammatory response of the IAs wall plays a crucial role in the progression of the IAs wall from a stable state to an unstable state [6, 28, 29]. This study may suggest that a sustained inflammatory response of the symptomatic aneurysm wall accompanies increased permeability (or remodeling of the IAs wall). The observed disparity in the OR values between K^{trans} and WEI in the final model implies that the augmentation of permeability in symptomatic aneurysm walls might be comparatively less pronounced than the enhancement of inflammatory response. Moreover, the different metric units of K^{trans} and WEI should be noticed. We also found that combining K^{trans} and WEI improved the reliability of identifying symptomatic aneurysms with a higher AUC than WEI alone.

Unlike previous DCE-MRI studies that directly segmented aneurysm wall regions on luminal imaging [10, 12, 20], our study segmented the IA wall using VWI to generate the corresponding K^{trans} on the co-registered DCE-MRI images. This approach allows for more accurate segmentation of vessel wall regions. The repeatability of this method was excellent. Unlike the previous permeability model [9], we applied the conventional Toft model in our study, a more commonly used method in clinical DCE studies. The above reasons may explain the differences in K^{trans} between our analysis and previous studies. In addition, the false inclusion of voxels containing lumens and selection of the highest K^{trans} rather than the average may also explain significant differences in K^{trans} compared with other studies.

Limitations

Our study has several limitations. Firstly, the data were obtained from a single tertiary center and thus may be subject to selection bias. Secondly, this study lacked dynamic observation of the natural evolution of IAs to clarify the corresponding changes in K^{trans} and AWE. Future longitudinal studies are needed to confirm whether K^{trans} can predict IA growth or rupture. Thirdly, we obtained K^{trans} using the conventional permeability model, whereas the optimized permeability model may reflect permeability changes in IA walls more realistically. Fourthly, the absence of 3D analysis for aneurysm wall's AWE and K^{trans} is also our limitation. Finally, the generalizability of the results is limited since the reference K^{trans} values of normal vessel walls and choroid plexus are not provided. Others cannot directly use the absolute value of K^{trans} in this study due to variations in protocols/processing.

Conclusions

K^{trans} from DCE-MRI perfusion is associated with symptomatic aneurysms and aneurysm wall enhancement. K^{trans} and WEI perform better than traditional risk factors, such as size and PHASES score, for differentiating symptomatic from asymptomatic aneurysms.

Supplementary Material

Refer to Web version on PubMed Central for supplementary material.

Acknowledgements

We thank Dr. Jinxia Zhu and Feifei Qu of Siemens Healthineers Ltd for supporting MRI sequence debugging, data post-processing, and article polishing.

We sincerely thank all the patients and healthcare workers who participated in this study.

Funding

This study has received funding from the National Natural Science Foundation of China (Grant 82202105) and the Joint construction project in Henan Province (Grant LHGJ20220406). Chengcheng Zhu was supported by grants R01HL162743 and R00HL136883 from the United States National Institute of Health (NIH).

Abbreviations

AUC	Area under the curve
AWE	Aneurysmal wall enhancement
AWEP	Aneurysmal wall enhancement pattern
CI	Confidence interval
DCE-MRI	Dynamic contrast-enhanced magnetic resonance imaging
FOV	The field of view
IAs	Intracranial aneurysms
K^{trans}	The volume transfer constant
OR	Odds ratio
ROI	Region of interest
Rs	Spearman’s coefficient of rank correlation
SAH	Subarachnoid hemorrhage
SD	Standard deviation
SI	Signal intensity
SPACE	Fast-spin-echo with variable flip angle trains
TOF MRA	Time-of-flight magnetic resonance angiography
UIAs	Unruptured intracranial aneurysms
VFA	Variable flip angle
VIBE	Volumetric interpolated breathhold
VIF	Variance inflation factor
VOI	Volume of interest
VWI	Vessel wall magnetic resonance imaging

WEI	Wall enhancement index

References

1. Vernooij MW, Ikram MA, Tanghe HL et al. (2007) Incidental findings on brain MRI in the general population. N Engl J Med 357:1821–1828 [PubMed: 17978290]
2. Wang Y, Cheng M, Liu S et al. (2022) Shape related features of intracranial aneurysm are associated with rupture status in a large Chinese cohort. J Neurointerv Surg 14:252–256 [PubMed: 33883209]
3. Juvela S (2022) PHASES score and treatment scoring with cigarette smoking in the long-term prediction of rupturing of unruptured intracranial aneurysms. J Neurosurg 136:156–162 [PubMed: 34243151]
4. Wermer MJH, van der Schaaf IC, Algra A, Rinkel GJE (2007) Risk of rupture of unruptured intracranial aneurysms in relation to patient and aneurysm characteristics: an updated meta-analysis. Stroke 38:1404–1410 [PubMed: 17332442]
5. Fu Q, Wang Y, Zhang Y et al. (2021) Qualitative and quantitative wall enhancement on magnetic resonance imaging is associated with symptoms of unruptured intracranial aneurysms. Stroke 52:213–222 [PubMed: 33349014]
6. Morel S, Bijlenga P, Kwak BR (2022) Intracranial aneurysm wall (in)stability-current state of knowledge and clinical perspectives. Neurosurg Rev 45:1233–1253 [PubMed: 34743248]
7. Frösen J (2014) Smooth muscle cells and the formation, degeneration, and rupture of saccular intracranial aneurysm wall–a review of current pathophysiological knowledge. Transl Stroke Res 5:347–356 [PubMed: 24683005]
8. Zhong W, Su W, Li T et al. (2021) Aneurysm wall enhancement in unruptured intracranial aneurysms: a histopathological evaluation. J Am Heart Assoc 10:e018633 [PubMed: 33410330]
9. Cantrell CG, Vakil P, Jeong Y, Ansari SA, Carroll TJ (2017) Diffusion-compensated tofts model suggests contrast leakage through aneurysm wall. Magn Reson Med 78:2388–2398 [PubMed: 28112862]
10. Qi H, Liu X, Liu P et al. (2019) Complementary roles of dynamic contrast-enhanced MR imaging and postcontrast vessel wall imaging in detecting high-risk intracranial aneurysms. AJNR Am J Neuroradiol 40:490–496 [PubMed: 30792252]
11. Edjlali M, Guédon A, Ben Hassen W et al. (2018) Circumferential thick enhancement at vessel wall MRI has high specificity for intracranial aneurysm instability. Radiology 289:181–187 [PubMed: 29969070]
12. Vakil P, Ansari SA, Cantrell CG et al. (2015) Quantifying intracranial aneurysm wall permeability for risk assessment using dynamic contrast-enhanced MRI: a pilot study. AJNR Am J Neuroradiol 36:953–959 [PubMed: 25655875]
13. Tóth A (2023) Wall enhancement in stable aneurysms needs to be understood first to be able to identify instable and culprit aneurysms. Eur Radiol 33:4915–4917 [PubMed: 37212849]
14. Molenberg R, Aalbers MW, Appelman APA, Uyttenboogaart M, van Dijk JMC (2021) Intracranial aneurysm wall enhancement as an indicator of instability: a systematic review and meta-analysis. Eur J Neurol 28:3837–3848
15. Matsushige T, Shimonaga K, Ishii D et al. (2019) Vessel wall imaging of evolving unruptured intracranial aneurysms. Stroke 50:1891–1894 [PubMed: 31167619]
16. Greving JP, Wermer MJH, Brown RD et al. (2014) Development of the PHASES score for prediction of risk of rupture of intracranial aneurysms: a pooled analysis of six prospective cohort studies. Lancet Neurol 13:59–66 [PubMed: 24290159]
17. O'brien RM (2007) Quality & Quantity. A caution regarding rules of thumb for variance inflation factors. Qual Quant 41:673–690
18. Ball MJ (1975) Pathogenesis of the "sentinel headache" preceding berry aneurysm rupture. Can Med Assoc J 112:78–79 [PubMed: 1109729]
19. Nakagawa D, Kudo K,Awe O et al. (2018) Detection of microbleeds associated with sentinel headache using MRI quantitative susceptibility mapping: pilot study. J Neurosurg 10.3171/2018.2.JNS1884:1-7

20. Wang Y, Sun J,Li R et al. (2022) Increased aneurysm wall permeability colocalized with low wall shear stress in unruptured saccular intracranial aneurysm. J Neurol 269:2715–2719 [PubMed: 34731309]
21. Peng F, Niu H,Feng X et al. (2023) Aneurysm wall enhancement, atherosclerotic proteins, and aneurysm size may be related in unruptured intracranial fusiform aneurysms. Eur Radiol 33:4918–4926 [PubMed: 36840766]
22. Kang H, Tian D-C,Yang X et al. (2022) A randomized controlled trial of statins to reduce inflammation in unruptured cerebral aneurysms. JACC Cardiovasc Imaging 15:1668–1670 [PubMed: 36075628]
23. Quan K, Song J,Yang Z et al. (2019) Validation of wall enhancement as a new imaging biomarker of unruptured cerebral aneurysm. Stroke 50:1570–1573 [PubMed: 31035900]
24. Meng H, Tutino VM,Xiang J, Siddiqui A (2014) High WSS or low WSS? Complex interactions of hemodynamics with intracranial aneurysm initiation, growth, and rupture: toward a unifying hypothesis. AJNR Am J Neuroradiol 35:1254–1262 [PubMed: 23598838]
25. Etminan N, Rinkel GJ (2016) Unruptured intracranial aneurysms: development, rupture and preventive management. Nat Rev Neurol 12:699–713 [PubMed: 27808265]
26. Zhu C, Wang X, Eisenmenger L et al. (2020) Wall enhancement on blackblood MRI is independently associated with symptomatic status of unruptured intracranial saccular aneurysm. Eur Radiol 30:6413–6420 [PubMed: 32666320]
27. Peng F, Fu M, Xia J et al. (2022) Quantification of aneurysm wall enhancement in intracranial fusiform aneurysms and related predictors based on high-resolution magnetic resonance imaging: a validation study. Ther Adv Neurol Disord 15:17562864221105342
28. Ge P, Liu C, Chan L et al. (2022) High-dimensional immune profiling by mass cytometry revealed the circulating immune cell landscape in patients with intracranial aneurysm. Front Immunol 13:922000 [PubMed: 35833148]
29. Chalouhi N, Hoh BL, Hasan D et al. (2013) Review of cerebral aneurysm formation, growth, and rupture. Stroke 44:3613–3622 [PubMed: 24130141]

Key Points

- The volume transfer constant is correlated with intracranial aneurysm symptoms and aneurysmal wall enhancement.
- Dynamic contrast-enhanced and vessel wall MRI facilitates understanding of the pathophysiological characteristics of intracranial aneurysm walls.
- The volume transfer constant and wall enhancement index perform better than the traditional PHASES score in differentiating symptomatic aneurysms.

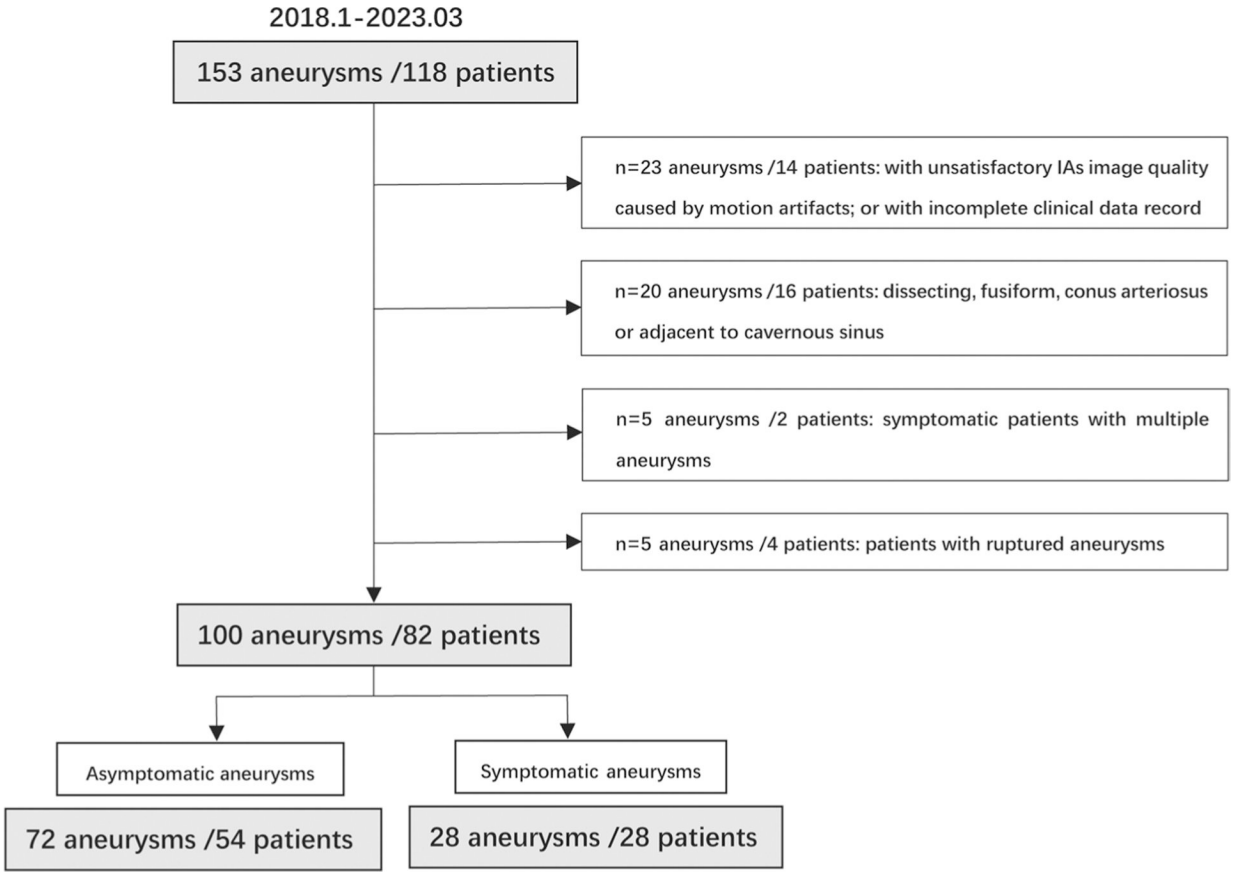

Fig. 1.
Flowchart of the patient selection process

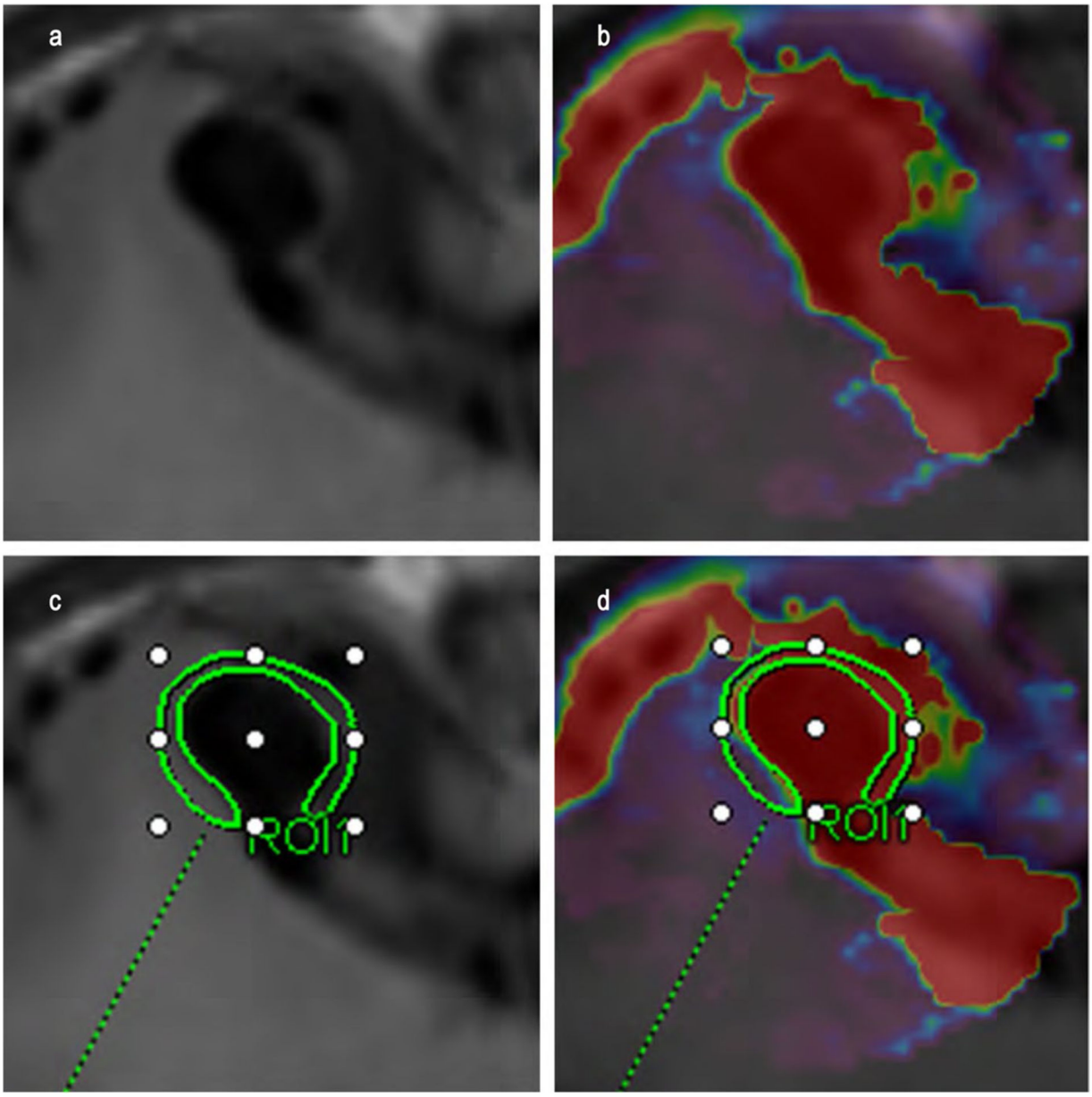

Fig. 2.

Example case for image processing. **a**, **b** Original images. **c**, **d** Contours of the aneurysmal wall. **a** and **c** show the postcontrast vessel wall images (VWI) on which the outline of the region of interest (ROI) was traced manually, and **b** and **d** show the dynamic contrast-enhanced MRI (DCE-MRI) on which the VWI and contour of the ROI were matched automatically

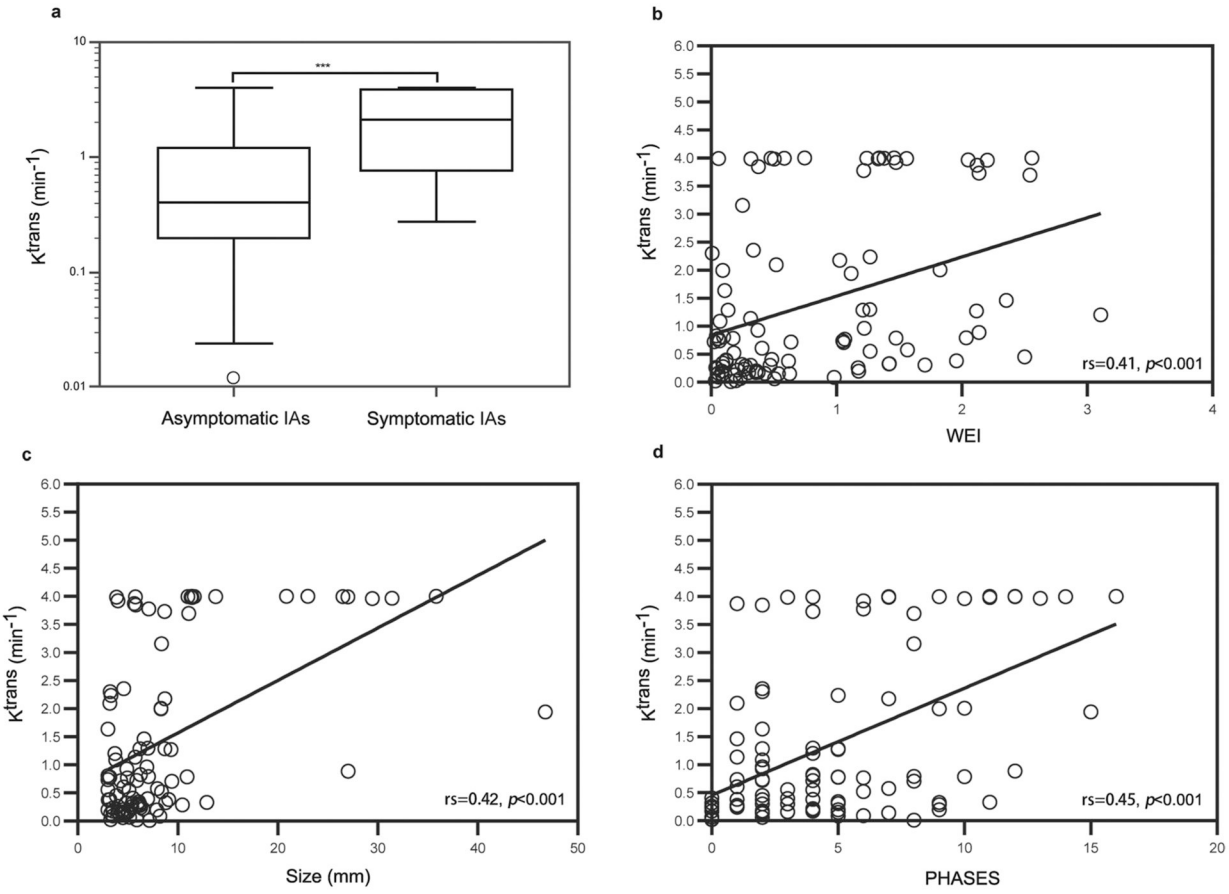

Fig. 3.

Boxplot of K^{trans} on asymptomatic and symptomatic aneurysms (**a**). Plots showing the relationships between K^{trans} and wall enhancement index (WEI) (**b**), aneurysm size (**c**), and PHASES score (**d**). ***$p < 0.001$, Spearman's coefficient of rank correlation (rs)

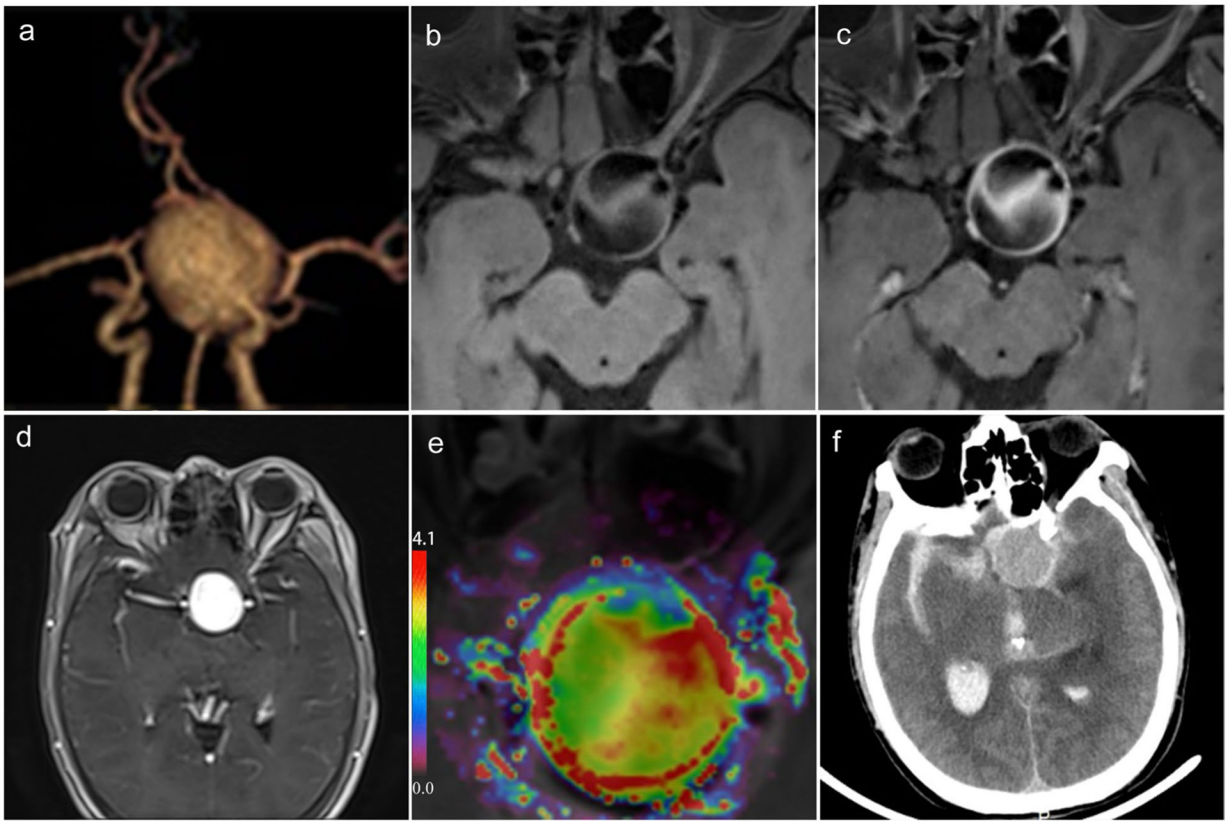

Fig. 4.

The evolution of a symptomatic aneurysm demonstrates that elevated K^{trans} at baseline was correlated with a rupture. **a** CT angiography of a 44-year-old man with oculomotor nerve palsy and an aneurysm on the left internal carotid artery terminal, measuring 27 mm. **b**, **c** Pre/postcontrast VWI (T1WI-fat saturation) of the aneurysm (AWEP 2). **d** Original DCE-MRI image. **e** Pseudo-color map of K^{trans} on the DCE-MRI of the aneurysm (K^{trans} = 4.0 min^{-1}). **f** CT showing eventual SAH day 6 after baseline scan

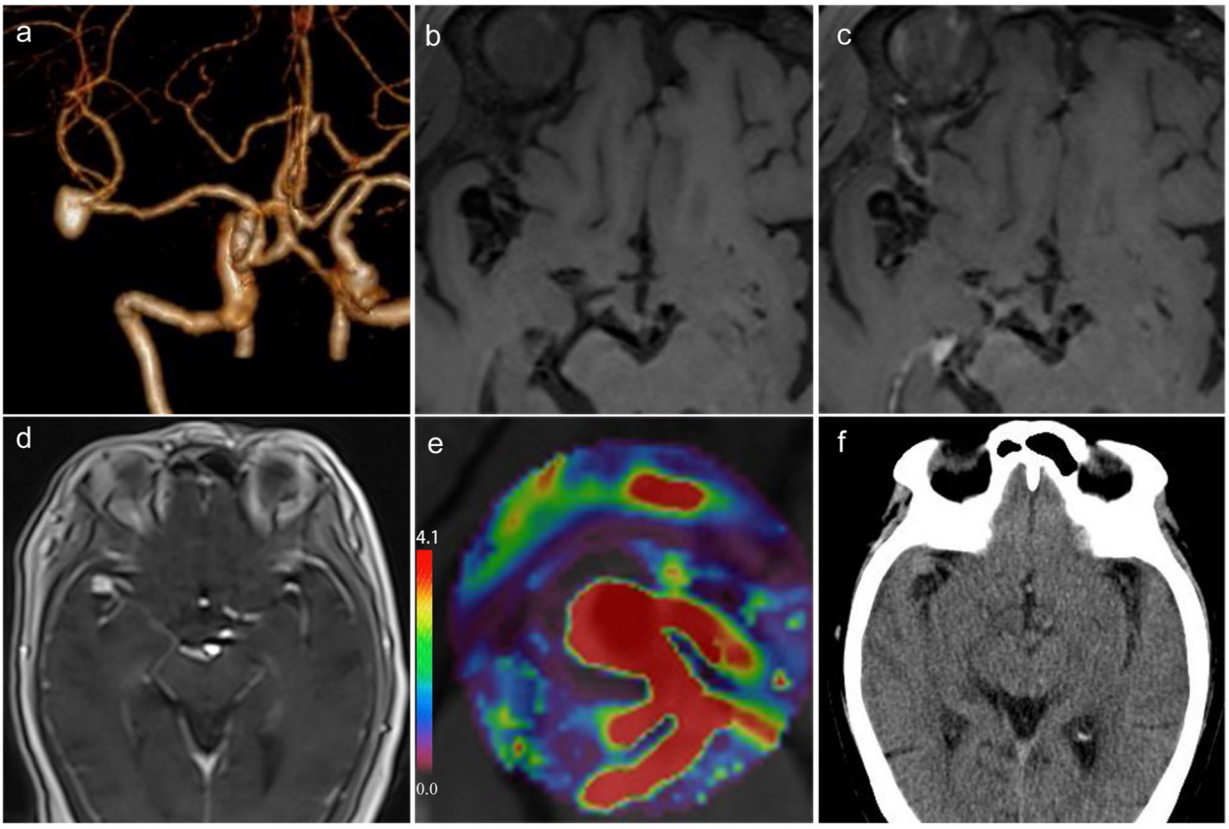

Fig. 5.

Representative case of asymptomatic intracranial aneurysm. **a** CT angiography of a 73-year-old woman with no symptoms and an aneurysm on the right middle cerebral artery measuring 9.4 mm. **b**, **c** Pre/postcontrast VWI (T1WI-fat saturation) of the aneurysm (AWEP 2). **d** Original DCE-MRI image. **e** Pseudo-color map of K^{trans} on the DCE-MRI of the aneurysm (K^{trans} = 0.7 min^{-1}). **f** CT showing no SAH at baseline scan

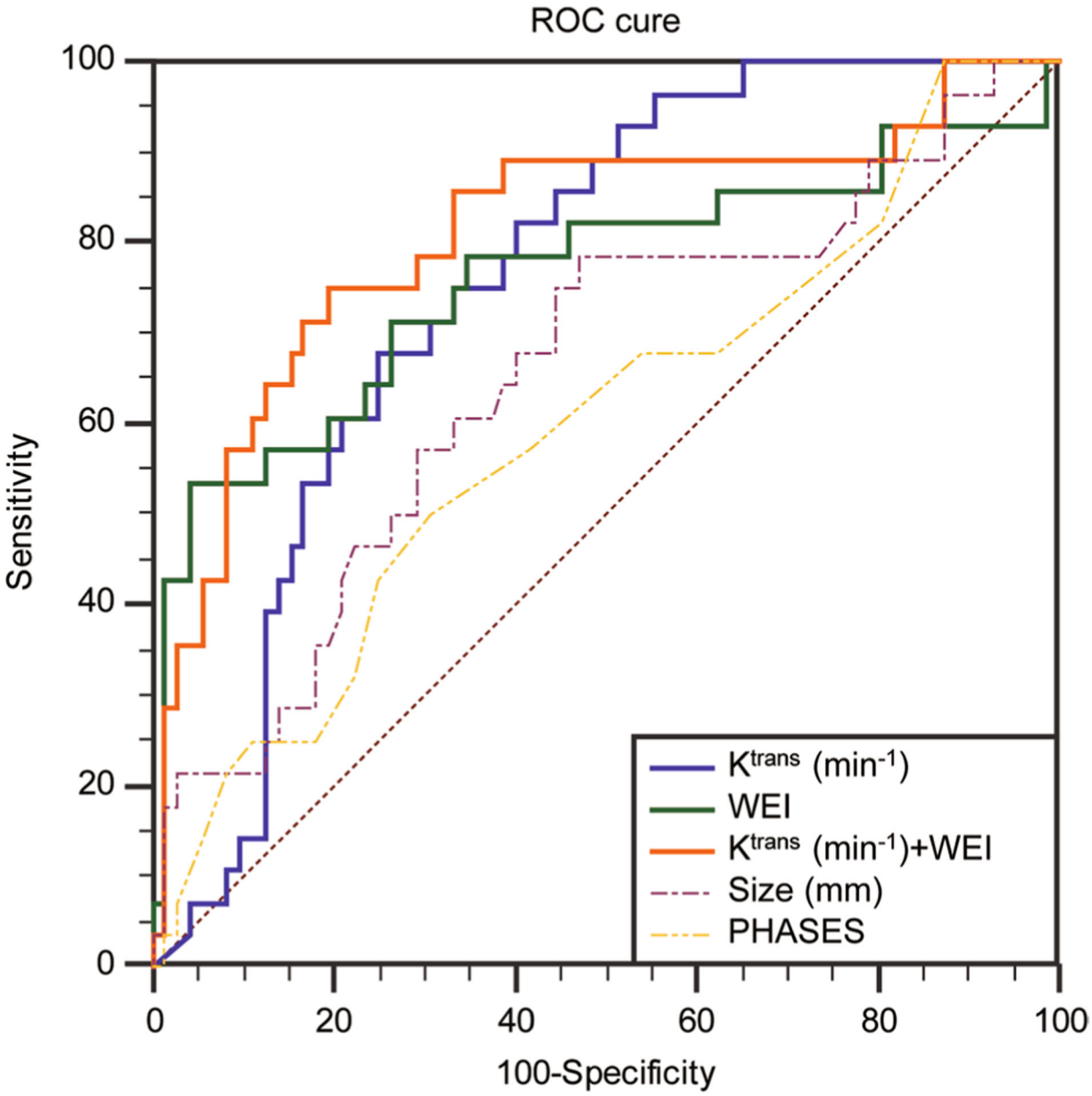

Fig. 6.

Receiver operating characteristic (ROC) curves of aneurysm characters for differentiating symptomatic and asymptomatic intracranial aneurysms. The AUCs for K^{trans}, WEI, K^{trans} + WEI, size, and PHASES were 0.76, 0.76, 0.81, 0.66, and 0.59, respectively

Table 1

Demographics and aneurysm characteristics

Parameter	Total (*n* = 100)	Asymptomatic aneurysms (*n* = 72)	Symptomatic aneurysms (*n* = 28)	*p*-value
Age (y)	58.2 ± 10.5	59.5 ± 9.6	54.8 ± 11.9	0.11
Female sex	70 (70.0)	47 (65.3)	23 (82.1)	0.16
Hypertension	52 (52.0)	39 (54.2)	13 (46.4)	0.49
Dyslipidemia	41 (41.0)	30 (41.7)	11 (39.3)	0.83
Diabetes	10 (10.0)	5 (6.9)	5 (17.9)	0.10
Previous SAH	4 (4.0)	4 (5.6)	0 (0.0)	0.21
Cigarette smoking	13 (13.0)	11 (15.3)	2 (7.1)	0.28
Alcohol consumption	15 (15.0)	14 (19.4)	1 (3.6)	0.05
Aspirin intake	13 (13.0)	13 (18.1)	0 (0.0)	0.02 *
Family history of aneurysm	11 (11.0)	7 (9.7)	4 (14.3)	0.52
Anterior circulation	90 (90.0)	64 (88.9)	26 (92.9)	0.56
Aneurysm size (mm)	5.9 (4.0, 8.7)	5.4 (4.0, 8.3)	7.5 (5.7, 11.2)	0.02 *
AWEP				< 0.001 *
AWEP 0	55 (55.0)	48 (66.7)	7 (25.0)	
AWEP 1	20 (20.0)	15 (20.8)	5 (17.9)	
AWEP 2	25 (25.0)	9 (12.5)	16 (57.1)	
WEI	0.5 (0.2, 1.3)	0.4 (0.1, 1.1)	1.5 (0.6, 2.1)	< 0.001 *
K^{trans} (min^{-1})	0.7 (0.3, 2.2)	0.4 (0.2, 1.2)	2.1 (0.8, 3.9)	< 0.001 *
PHASES score	4.0 (2.0, 7.5)	4.0 (2.0, 6.5)	5.5 (2.0, 9.0)	0.13

Continuous variables are presented as the mean ± SD or median (interquartile range) as appropriate. The *n* (%) represents categorical variables. *SAH*, subarachnoid hemorrhage; *AWEP*, aneurysmal wall enhancement patterns; *WEI*, wall enhancement index; K^{trans}, the volume transfer constant

*Statistically significant

Table 2

Logistic mixed effect regression for factors associated with aneurysms in patients with symptoms

Variables	Univariate analysis			Multivariate analysis		
	***p*-value**	**OR**	**95%CI**	***p*-value**	**OR**	**95%CI**
Age	0.04*	0.96	0.92–0.99	0.14	0.95	0.90–1.02
Female	0.11	2.45	0.83–7.22	NA		
Diabetes	0.11	2.91	0.77–10.98	NA		
Previous SAH	1	NA		NA		
Alcohol consumption	0.08	0.15	0.02–1.23	NA		
Aspirin intake	1	NA		NA		
Aneurysm size (mm)	0.01*	1.08	1.02–1.15	0.68	0.98	0.89–1.08
AWEP	< 0.001*	3.49	1.96–6.22	0.64	1.29	0.45–3.73
WEI	< 0.001*	4.66	2.33–9.34	0.04*	3.31	1.05–10.42
K^{trans} (s^{-1})	< 0.001*	1.77	1.30–2.40	0.04*	1.60	1.01–2 2.52
PHASES score	0.10	1.10	0.98–1.23	NA		

NA, no results for the model analysis; *OR*, odds ratio; *CI*, confidence interval; *SAH*, subarachnoid hemorrhage; *AWEP*, aneurysmal wall enhancement patterns; *WEI*, wall enhancement index; K^{trans}, the volume transfer constant

*Statistically significant

Table 3

ROC curve characteristics for differentiating symptomatic from asymptomatic aneurysms

Variables	AUC	Sensitivity (%)	Specificity (%)	Youden index
K^{trans}	0.76	67.86	75.00	0.43
WEI	0.76	53.57	95.83	0.49
K^{trans} + WEI	0.81	75.00	80.56	0.56
Aneurysm size	0.66	78.57	52.78	0.31
PHASES	0.59	50.00	69.44	0.19

ROC, receiver operating characteristic; *AUC*, the area under the ROC curve; *WEI*, wall enhancement index; K^{trans}, the volume transfer constant

*Statistically significant